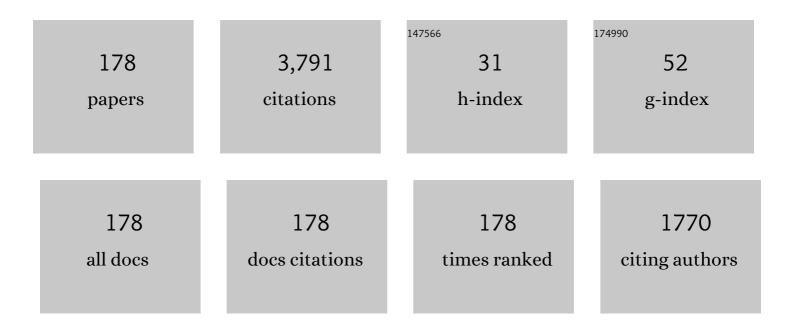
Rodney Badcock

List of Publications by Year in descending order

Source: https://exaly.com/author-pdf/7285888/publications.pdf Version: 2024-02-01



#	Article	IF	CITATIONS
1	High power density superconducting rotating machines—development status and technology roadmap. Superconductor Science and Technology, 2017, 30, 123002.	1.8	309
2	Dynamic resistance of a high- <i>Tc</i> superconducting flux pump. Applied Physics Letters, 2014, 105, .	1.5	138
3	Triboluminescent damage sensors. Smart Materials and Structures, 1999, 8, 504-510.	1.8	122
4	VIPER: an industrially scalable high-current high-temperature superconductor cable. Superconductor Science and Technology, 2020, 33, 11LT01.	1.8	114
5	The use of 0-3 piezocomposite embedded Lamb wave sensors for detection of damage in advanced fibre composites. Smart Materials and Structures, 2000, 9, 291-297.	1.8	96
6	Development of a brushless HTS exciter for a 10 kW HTS synchronous generator. Superconductor Science and Technology, 2016, 29, 024008.	1.8	96
7	Anomalous open-circuit voltage from a high- <i>T</i> c superconducting dynamo. Applied Physics Letters, 2016, 108, .	1.5	85
8	Impact of flux gap upon dynamic resistance of a rotating HTS flux pump. Superconductor Science and Technology, 2015, 28, 115008.	1.8	84
9	Fabrication of intrinsic fibre Fabry–Perot sensors in silica fibres using hydrofluoric acid etching. Sensors and Actuators A: Physical, 2007, 138, 248-260.	2.0	81
10	Progress in the Manufacture of Long Length YBCO Roebel Cables. IEEE Transactions on Applied Superconductivity, 2009, 19, 3244-3247.	1.1	78
11	Methodology and integrity monitoring of foundation concrete piles using Bragg grating optical fibre sensors. Engineering Structures, 2007, 29, 2048-2055.	2.6	71
12	A novel ultrasound fibre optic sensor based on a fused-tapered optical fibre coupler. Measurement Science and Technology, 2004, 15, 1490-1495.	1.4	70
13	Optimizing the sensitivity of palladium based hydrogen sensors. Sensors and Actuators B: Chemical, 2018, 259, 10-19.	4.0	59
14	Through-Wall Excitation of a Magnet Coil by an External-Rotor HTS Flux Pump. IEEE Transactions on Applied Superconductivity, 2016, 26, 1-5.	1.1	58
15	An intensity-based optical fibre sensor for fatigue damage detection in advanced fibre-reinforced composites. Smart Materials and Structures, 1995, 4, 223-230.	1.8	53
16	Narrow strand YBCO Roebel cable for lowered AC loss. Journal of Physics: Conference Series, 2008, 97, 012280.	0.3	52
17	Origin of the DC output voltage from a high- <i>Tc</i> superconducting dynamo. Applied Physics Letters, 2019, 114, .	1.5	51
18	Design and Performance of a "Squirrel-Cage―Dynamo-Type HTS Flux Pump. IEEE Transactions on Applied Superconductivity, 2018, 28, 1-5.	1.1	47

#	Article	IF	CITATIONS
19	Impact of <bold>S</bold> tator Wire Width on Output of a Dynamo-Type HTS Flux Pump. IEEE Transactions on Applied Superconductivity, 2016, 26, 1-8.	1.1	44
20	Fiber optic quench detection for large-scale HTS magnets demonstrated on VIPER cable during high-fidelity testing at the SULTAN facility. Superconductor Science and Technology, 2021, 34, 035027.	1.8	43
21	Development of YBCO Roebel cables for high current transport and low AC loss applications. Journal of Physics: Conference Series, 2010, 234, 022021.	0.3	40
22	Frequency Dependent Behavior of a Dynamo-Type HTS Flux Pump. IEEE Transactions on Applied Superconductivity, 2017, 27, 1-5.	1.1	39
23	Maximising the current output from a self-switching kA-class rectifier flux pump. Superconductor Science and Technology, 2020, 33, 045005.	1.8	39
24	A Novel Rotating HTS Flux Pump Incorporating a Ferromagnetic Circuit. IEEE Transactions on Applied Superconductivity, 2016, 26, 84-89.	1.1	37
25	AC loss simulation in a HTS 3-Phase 1â€ ⁻ MVA transformer using H formulation. Cryogenics, 2018, 94, 14-21.	0.9	37
26	Impact of Magnet Geometry on Output of a Dynamo-Type HTS Flux Pump. IEEE Transactions on Applied Superconductivity, 2017, 27, 1-5.	1.1	35
27	Mechanism of the High- <mml:math <br="" xmlns:mml="http://www.w3.org/1998/Math/MathML">display="inline" overflow="scroll"><mml:msub><mml:mi>T</mml:mi><mml:mi>c</mml:mi></mml:msub></mml:math> Superconducting Dynamo: Models and Experiment, Physical Review Applied, 2020, 14, .	1.5	34
28	Design of a single-phase 6.5 MVA/25ÂkV superconducting traction transformer for the Chinese Fuxing high-speed train. International Journal of Electrical Power and Energy Systems, 2020, 119, 105956.	3.3	33
29	The transient voltage response of ReBCO coated conductors exhibiting dynamic resistance. Superconductor Science and Technology, 2020, 33, 035007.	1.8	33
30	Structural health monitoring of a composite bridge using Bragg grating sensors. Part 1: Evaluation of adhesives and protection systems for the optical sensors. Engineering Structures, 2007, 29, 440-448.	2.6	31
31	Transport AC loss characteristics of a nine strand YBCO Roebel cable. Superconductor Science and Technology, 2010, 23, 025028.	1.8	31
32	The development of a Roebel cable based 1 MVA HTS transformer. Superconductor Science and Technology, 2012, 25, 014002.	1.8	31
33	Test Results and Conclusions From a 1 MVA Superconducting Transformer Featuring 2G HTS Roebel Cable. IEEE Transactions on Applied Superconductivity, 2017, 27, 1-5.	1.1	31
34	A multi-mode extrinsic Fabry - Pérot interferometric strain sensor. Smart Materials and Structures, 1997, 6, 464-469.	1.8	30
35	Transport AC loss measurement of a five strand YBCO Roebel cable. Superconductor Science and Technology, 2009, 22, 095002.	1.8	30
36	Coupling time constants of striated and copper-plated coated conductors and the potential of striation to reduce shielding-current-induced fields in pancake coils. Superconductor Science and Technology, 2018, 31, 025007.	1.8	30

#	Article	IF	CITATIONS
37	Monitoring of an all-composite bridge using Bragg grating sensors. Construction and Building Materials, 2007, 21, 1599-1604.	3.2	29
38	Magnetic AC Loss Characteristics of 2G Roebel Cable. IEEE Transactions on Applied Superconductivity, 2009, 19, 3361-3364.	1.1	28
39	Design and Heat Load Analysis of a 12 MW HTS Wind Power Generator Module Employing a Brushless HTS Exciter. IEEE Transactions on Applied Superconductivity, 2016, 26, 1-4.	1.1	28
40	AC loss measurements in pancake coils wound with 2G tapes and Roebel cable: dependence on spacing between turns/strands. Superconductor Science and Technology, 2012, 25, 035002.	1.8	27
41	Superconducting AC Homopolar Machines for High-Speed Applications. Energies, 2019, 12, 86.	1.6	27
42	A novel optical fiber-based strain sensor. IEEE Photonics Technology Letters, 1997, 9, 982-984.	1.3	26
43	Dynamic Resistance Measurements in a GdBCO-Coated Conductor. IEEE Transactions on Applied Superconductivity, 2017, 27, 1-5.	1.1	26
44	Dynamic Resistance Measurement of a Four-Tape YBCO Stack in a Perpendicular Magnetic Field. IEEE Transactions on Applied Superconductivity, 2018, 28, 1-5.	1.1	26
45	The dependence of AC loss characteristics on the spacing between strands in YBCO Roebel cables. Superconductor Science and Technology, 2011, 24, 065005.	1.8	25
46	Palladium-Based Hydrogen Sensors Using Fiber Bragg Gratings. Journal of Lightwave Technology, 2018, 36, 850-856.	2.7	25
47	Total loss measurement and simulation in a REBCO coated conductor carrying DC current in perpendicular AC magnetic field at various temperatures. Superconductor Science and Technology, 2021, 34, 065009.	1.8	25
48	A multi-purpose optical fibre sensor design for fibre reinforced composite materials. Measurement Science and Technology, 1997, 8, 1065-1079.	1.4	24
49	Comparison of transport AC losses in an eight-strand YBCO Roebel cable and a four-tape YBCO stack. Physica C: Superconductivity and Its Applications, 2011, 471, 999-1002.	0.6	24
50	AC loss measurements in HTS coil assemblies with hybrid coil structures. Superconductor Science and Technology, 2016, 29, 095011.	1.8	24
51	Finite-element modelling of no-insulation HTS coils using rotated anisotropic resistivity. Superconductor Science and Technology, 2020, 33, 08LT01.	1.8	24
52	Frequency dependence of magnetic ac loss in a Roebel cable made of YBCO on a Ni–W substrate. Superconductor Science and Technology, 2010, 23, 085009.	1.8	23
53	Motors Employing REBCO CORC and MgB ₂ Superconductors for AC Stator Windings. IEEE Transactions on Applied Superconductivity, 2021, 31, 1-7.	1.1	23
54	Modeling of Stator Versus Magnet Width Effects in High-\$T_c\$ Superconducting Dynamos. IEEE Transactions on Applied Superconductivity, 2020, 30, 1-6.	1.1	22

#	Article	IF	CITATIONS
55	Selecting of FBG Coatings for Quench Detection in HTS Coils. IEEE Transactions on Applied Superconductivity, 2018, 28, 1-5.	1.1	21
56	High-Sensitivity Fiber-Optic Sensor for Hydrogen Detection in Gas and Transformer Oil. IEEE Sensors Journal, 2019, 19, 3348-3357.	2.4	21
57	Superconducting rotating machines for aerospace applications. , 2018, , .		20
58	AC Loss Effect of High-Order Harmonic Currents in a Single-Phase 6.5 MVA HTS Traction Transformer. IEEE Transactions on Applied Superconductivity, 2019, 29, 1-5.	1.1	20
59	The scaling of transport AC losses in Roebel cables with varying strand parameters. Superconductor Science and Technology, 2014, 27, 075007.	1.8	19
60	Electromagnetic Characteristic Analysis and Optimization Design of a Novel HTS Coreless Induction Motor For High-Speed Operation. IEEE Transactions on Applied Superconductivity, 2018, 28, 1-5.	1.1	19
61	A Wireless Rectifier for Inductively Energizing High Direct-Current High-Temperature Superconducting Magnets. IEEE Transactions on Industrial Electronics, 2021, 68, 3273-3281.	5.2	19
62	15% reduction in AC loss of a 3-phase 1 MVA HTS transformer by exploiting asymmetric conductor critical current. Journal of Physics Communications, 2021, 5, 025003.	0.5	19
63	A half-wave superconducting transformer-rectifier flux pump using J _c (B) switches. Superconductor Science and Technology, 2022, 35, 035009.	1.8	19
64	Current carrying capability of HTS Roebel cable. Physica C: Superconductivity and Its Applications, 2011, 471, 42-47.	0.6	18
65	Total AC loss measurements in a six strand Roebel cable carrying an AC current in an AC magnetic field. Superconductor Science and Technology, 2013, 26, 035014.	1.8	18
66	Mode I Delamination Testing of REBCO Coated Conductors via Climbing Drum Peel Test. IEEE Transactions on Applied Superconductivity, 2018, 28, 1-5.	1.1	18
67	Optimizing Rotor Speed and Geometry for an Externally Mounted HTS Dynamo. IEEE Transactions on Applied Superconductivity, 2019, 29, 1-5.	1.1	18
68	Frequency dependence of magnetic ac loss in a five strand YBCO Roebel cable. Superconductor Science and Technology, 2010, 23, 065008.	1.8	17
69	Output During Continuous Frequency Ramping of a Dynamo-Type HTS Flux Pump. IEEE Transactions on Applied Superconductivity, 2018, 28, 1-5.	1.1	17
70	Improving the Sensitivity of Palladium-Based Fiber Optic Hydrogen Sensors. Journal of Lightwave Technology, 2018, 36, 2166-2174.	2.7	17
71	Dynamic Resistance Measurement in a Four-Tape YBCO Stack With Various Applied Field Orientation. IEEE Transactions on Applied Superconductivity, 2019, 29, 1-7.	1.1	17
72	Design of a 12-MW HTS Wind Power Generator Including a Flux Pump Exciter. IEEE Transactions on Applied Superconductivity, 2016, 26, 1-5.	1.1	16

#	Article	IF	CITATIONS
73	Critical current retention of potted and unpotted REBCO Roebel cables under transverse pressure and thermal cycling. Superconductor Science and Technology, 2017, 30, 045014.	1.8	16
74	AC Loss Characteristics in REBCO Coil Assemblies With Different Geometries and Conductors. IEEE Transactions on Applied Superconductivity, 2018, 28, 1-5.	1.1	16
75	Dynamic resistance measurement in a YBCO wire under perpendicular magnetic field at various operating temperatures. Journal of Applied Physics, 2019, 126, .	1.1	16
76	Simulation of AC Loss in the Armature Windings of a 100 kW All-HTS Motor With Various (RE)BCO Conductor Considerations. IEEE Access, 2021, 9, 130968-130980.	2.6	16
77	Design, Fabrication, and Analysis of HTS Coils for a 10-kW Wind Power Generator Employing a Brushless Exciter. IEEE Transactions on Applied Superconductivity, 2017, 27, 1-5.	1.1	15
78	A Superconducting Induction Motor with a High Temperature Superconducting Armature: Electromagnetic Theory, Design and Analysis. Energies, 2018, 11, 792.	1.6	15
79	Exploiting asymmetric wire critical current for the reduction of AC loss in HTS coil windings. Journal of Physics Communications, 2019, 3, 095017.	0.5	15
80	Numerical Modelling of Dynamic Resistance in a Parallel-Connected Stack of HTS Coated-Conductor Tapes. IEEE Transactions on Applied Superconductivity, 2020, 30, 1-8.	1.1	15
81	Practical Estimation of HTS Dynamo Losses. IEEE Transactions on Applied Superconductivity, 2020, 30, 1-5.	1.1	14
82	AC loss measurement and simulation in a REBCO coil assembly utilising low-loss magnetic flux diverters. Superconductor Science and Technology, 2020, 33, 115011.	1.8	14
83	Experimental Comparison of AC Loss in REBCO Roebel Cables Consisting of Six Strands and Ten Strands. IEEE Transactions on Applied Superconductivity, 2014, 24, 1-5.	1.1	13
84	Monitoring Pre-Stressed Composites Using Optical Fibre Sensors. Sensors, 2016, 16, 777.	2.1	13
85	Experimental and numerical transport AC losses in a four-strand Roebel cable bifilar stack. Superconductor Science and Technology, 2018, 31, 115001.	1.8	13
86	Magnetic and Transport AC Losses in HTS Roebel Cable. IEEE Transactions on Applied Superconductivity, 2011, 21, 3311-3315.	1.1	12
87	AC Loss Measurements in a Hybrid REBCO/BSCCO Coil Assembly. IEEE Transactions on Applied Superconductivity, 2017, 27, 1-7.	1.1	12
88	Homopolar superconducting AC machines, with HTS dynamo driven field coils, for aerospace applications. IOP Conference Series: Materials Science and Engineering, 2020, 756, 012028.	0.3	12
89	Design of a 60 kA Flux Pump for Fusion Toroidal Field Coils. IEEE Transactions on Applied Superconductivity, 2022, 32, 1-5.	1.1	12
90	Effective reduction of magnetisation losses in copper-plated multifilament coated conductors using spiral geometry. Superconductor Science and Technology, 2022, 35, 025003.	1.8	12

#	Article	IF	CITATIONS
91	<title>Design, fabrication, and evaluation of an optical fiber sensor for tensile and compressive strain measurements via the use of white light interferometry</title> . , 1996, 2718, 408.		11
92	AC Loss Measurement in HTS Coil Windings Coupled With Iron Core. IEEE Transactions on Applied Superconductivity, 2019, 29, 1-5.	1.1	11
93	Asynchronous Magnet–Stator Topologies in a Squirrel-Cage Superconducting Dynamo. IEEE Transactions on Applied Superconductivity, 2019, 29, 1-5.	1.1	11
94	Propulsion motor concepts for airplanes. , 2019, , .		11
95	AC Loss Calculation on a 6.5 MVA/25 kV HTS Traction Transformer With Hybrid Winding Structure. IEEE Transactions on Applied Superconductivity, 2020, 30, 1-5.	1.1	11
96	Evaluation of continuous fiber Bragg grating and signal processing method for hotspot detection at cryogenic temperatures. Superconductor Science and Technology, 2022, 35, 054005.	1.8	11
97	Sensitive Fiber Optic Sensor for Rapid Hot-Spot Detection at Cryogenic Temperatures. IEEE Sensors Journal, 2022, 22, 11775-11782.	2.4	11
98	Role of Flux Diverters in Reducing AC Loss in a Single-Phase 6.5 MVA HTS Traction Transformer for Chinese High-Speed Train Carrying High-Order Harmonic Currents. IEEE Access, 2022, 10, 69650-69658.	2.6	11
99	Fabrication of intrinsic fibre Fabry–Perot cavities in silica optical fibres via F2-laser ablation. Measurement Science and Technology, 2007, 18, 928-934.	1.4	10
100	Fabrication, Qualification and Test of High \${m J}_{m c}\$ Roebel \${m YBa}_{2}{m Cu}_{3}{m O}_{7-delta}\$ Coated Conductor Cable for HEP Magnets. IEEE Transactions on Applied Superconductivity, 2011, 21, 2331-2334.	1.1	10
101	Impact of Annular Yoke Geometry on Performance of a Dynamo-Type HTS Flux Pump. IEEE Transactions on Applied Superconductivity, 2018, 28, 1-6.	1.1	10
102	Design and Performance Analysis of a Dynamo-Type HTS Flux Pump for a 10ÂkW Superconducting Generator. IEEE Transactions on Applied Superconductivity, 2020, 30, 1-5.	1.1	10
103	Stiffness Enhancement of a Superconducting Magnetic Bearing Using Shaped YBCO Bulks. IEEE Transactions on Applied Superconductivity, 2020, 30, 1-6.	1.1	10
104	A Rotating Flux Pump Employing a Magnetic Circuit and a Stabilized Coated Conductor HTS Stator. Journal of Magnetics, 2016, 21, 239-243.	0.2	10
105	Linear location of acoustic emission using a pair of novel fibre optic sensors. Journal of Physics: Conference Series, 2005, 15, 232-236.	0.3	9
106	Shielding of Perpendicular Magnetic Fields in Metal Layers of REBCO Superconducting Tapes and Roebel Cables. IEEE Transactions on Applied Superconductivity, 2018, 28, 1-8.	1.1	9
107	Shielding Effect of (RE)Ba ₂ Cu ₃ O _{7-d} -Coated Conductors on Eddy Current Loss of Adjacent Metal Layers Under AC Magnetic Fields With Various Orientations. IEEE Transactions on Applied Superconductivity, 2021, 31, 1-8.	1.1	9
108	Dynamic resistance and total loss in a three-tape REBCO stack carrying DC currents in perpendicular AC magnetic fields at 77 K. Superconductor Science and Technology, 2022, 35, 035011.	1.8	9

#	Article	IF	CITATIONS
109	Numerical Simulation of AC Loss in the Armature Windings of Two 50 Kw-Class All-HTS Motors With Different Pole Shapes. IEEE Transactions on Applied Superconductivity, 2022, 32, 1-7.	1.1	9
110	Impact of Copper Thickness, Conductor Width, and Number of Striations on Coupling Loss Characteristics of Copper-Plated Multifilament-Coated Conductors. IEEE Transactions on Applied Superconductivity, 2022, 32, 1-12.	1.1	9
111	<title>Squeezing light out of crystals: triboluminescent sensors</title> . , 1999, 3675, 169.		8
112	Magnetization Loss in REBCO Roebel Cables With Varying Strand Numbers. IEEE Transactions on Applied Superconductivity, 2018, 28, 1-5.	1.1	8
113	AC Loss Calculation of a Cosine-Theta Dipole Magnet Wound With Coated Conductors by 3D Modeling. IEEE Transactions on Applied Superconductivity, 2018, 28, 1-5.	1.1	8
114	The onset of dissipation in high-temperature superconductors: magnetic hysteresis and field dependence. Scientific Reports, 2018, 8, 14463.	1.6	8
115	Transport AC Loss Measurements in Bifilar Stacks Composed of YBCO-Coated Conductors. IEEE Transactions on Applied Superconductivity, 2018, 28, 1-6.	1.1	8
116	AC Losses in HTS Coils of Superferric Dipole and Combined-Function Magnets. IEEE Transactions on Applied Superconductivity, 2019, 29, 1-5.	1.1	8
117	Method for \$In-Situ\$ Strain Transfer Calibration of Surface Bonded Fiber Bragg Gratings. IEEE Sensors Journal, 2019, 19, 11926-11931.	2.4	8
118	Modelling Parallel-Connected, No-Insulation High-\${m T}_c\$ Superconducting Magnets. IEEE Transactions on Applied Superconductivity, 2021, 31, 1-5.	1.1	8
119	<title>Fatigue damage detection in carbon-fiber-reinforced composites using an intensity-based optical fiber sensor</title> . , 1995, 2444, 422.		7
120	Feasibility Study of Fiber Bragg Grating Sensor for Quench Detection of High Temperature Superconductors. IEEE Transactions on Applied Superconductivity, 2019, 29, 1-6.	1.1	7
121	Simplified Electromagnetic Modelling of Accelerator Magnets Wound With Conductor on Round Core Wires for AC Loss Calculations. IEEE Transactions on Applied Superconductivity, 2020, 30, 1-5.	1.1	7
122	Application of Epoxy-Bonded FBG Temperature Sensors for High-Temperature Superconductor-Coated Conductor Quench Detection. IEEE Transactions on Applied Superconductivity, 2021, 31, 1-8.	1.1	7
123	Role of asymmetric critical current on magnetization loss characteristics of (RE)Ba2Cu3O7â^' <i>d</i> coated conductors at various temperatures. Journal of Applied Physics, 2021, 130, .	1.1	7
124	Experimental and numerical study on AC loss reduction in a REBCO coil assembly by applying high saturation field powder-core flux diverters. Cryogenics, 2022, 124, 103466.	0.9	7
125	A novel technique to study the fracture of E-glass fiber reinforced composites. Journal of Materials Science, 2004, 39, 1425-1428.	1.7	6
126	Critical Current Behavior of HTS Roebel Cable Under Tensile Stress. IEEE Transactions on Applied Superconductivity, 2013, 23, 4801805-4801805.	1.1	6

#	Article	IF	CITATIONS
127	Characterization of Critical Current Distribution in Roebel Cable Strands Based on Reel-to-Reel Scanning Hall-Probe Microscopy. IEEE Transactions on Applied Superconductivity, 2017, 27, 1-4.	1.1	6
128	Design Improvisation for Reduced Harmonic Distortion in a Flux Pump-Integrated HTS Generator. Energies, 2017, 10, 1344.	1.6	6
129	Influence of E–J Characteristics of Coated Conductors and Field Ramp-Up Rates on Shielding-Current-Induced Fields of Magnet. IEEE Transactions on Applied Superconductivity, 2018, 28, 1-5.	1.1	6
130	Thermal Runaway of Conduction-Cooled Monofilament and Multifilament Coated Conductors. IEEE Transactions on Applied Superconductivity, 2022, 32, 1-9.	1.1	6
131	Current and Field Distribution in Meandered Coated Conductors for Roebel Cables. IEEE Transactions on Applied Superconductivity, 2011, 21, 3389-3392.	1.1	5
132	Solenoid Winding Using YBCO Roebel Cable. Physics Procedia, 2012, 36, 1159-1164.	1.2	5
133	Holistic approach for cryogenic cooling system design of 3 MW electrical aircraft motors. , 2021, , .		5
134	Application of Flux Diverters in High Temperature Superconducting Transformer Windings for AC Loss Reduction. IEEE Transactions on Applied Superconductivity, 2021, 31, 1-5.	1.1	5
135	Temperature Distribution in the Field Coil of a 500-kW HTS AC Homopolar Motor. IEEE Transactions on Applied Superconductivity, 2022, 32, 1-8.	1.1	5
136	Time-varying magnetic field induced electric field across a current-transporting type-II superconducting loop: beyond dynamic resistance effect. Superconductor Science and Technology, 2022, 35, 025018.	1.8	5
137	Transport AC Loss Characteristics of a Five Strand YBCO Roebel Cable With Magnetic Substrate. IEEE Transactions on Applied Superconductivity, 2011, 21, 3289-3292.	1.1	4
138	F2-laser ablation of Fabry–Perot cavities in optical fibres: chemical sensors. Journal of Optics (United) Tj ETQq	0 0 0 rgBT 1.0gBT	Oyerlock 10
139	The Dependence of Transport AC Loss on Temperature and DC Parallel Magnetic Field in an Eight-Strand YBCO Roebel Cable. IEEE Transactions on Applied Superconductivity, 2013, 23, 5402604-5402604.	1.1	4
140	Rapid synchronization procedure for a synchronous generator employing ballistic trajectory control. , 2016, , .		4
141	Development of hydrogen sensors based on fiber Bragg grating with a palladium foil for online dissolved gas analysis in transformers. , 2017, , .		4
142	Design analysis of a plasma thruster with superconducting magnets. , 2019, , .		4
143	Reducing Mission Cryogenic Load via HTS Dynamo. , 2020, , .		4
144	Reduction of AC Loss in HTS Coils of Superferric Magnets for Rapid-Cycling Synchrotrons by Changing Cross-Section of Coils and Iron Yoke Geometry. IEEE Transactions on Applied Superconductivity, 2020, 30, 1-5.	1,1	4

#	Article	IF	CITATIONS
145	Effect of Stack Geometry on the Dynamic Resistance Threshold Fields for Vertical Stacks of Coated Conductor Tapes. IEEE Transactions on Applied Superconductivity, 2021, 31, 1-4.	1.1	4
146	AC Loss Simulation in HTS Coil Windings Coupled With an Iron Core. IEEE Transactions on Applied Superconductivity, 2022, 32, 1-5.	1.1	4
147	<title>Distributed optical-fiber-based damage detection in composites</title> . , 1999, , .		3
148	FEM and performance analysis of 10 kW HTS generator with flux pump excitation. , 2016, , .		3
149	Test of Cryocooler-Cooled RE-123 Magnet on HIMAC Beam Line in S-Innovation Program. IEEE Transactions on Applied Superconductivity, 2019, 29, 1-5.	1.1	3
150	Coolant transfer coupling with integrated dynamo for rotor with HTS windings. IOP Conference Series: Materials Science and Engineering, 2020, 756, 012029.	0.3	3
151	Magnetic Field Drifts of Small HTS Dipole Magnet Under Repeated Excitation. IEEE Transactions on Applied Superconductivity, 2022, 32, 1-6.	1.1	3
152	Synthesis and characterization of a novel class of photo-actuating and photo-rheological polymers. , 2004, , .		2
153	Laser micromachined and acid-etched Fabry-Perot cavities in silica fibres. , 2005, , .		2
154	Analysis of remnant field detected by hall sensors above superconductor tape. , 2009, , .		2
155	Risk Mitigation in the Development of a Roebel Cable Based 1 MVA HTS Transformer. Physics Procedia, 2012, 36, 830-834.	1.2	2
156	Rapid synchronisation procedure for a pneumo-hydraulically driven synchronous generator. , 2017, , .		2
157	Influence of fluid selection on synchronous generators power output in compressed air energy storage systems. , 2017, , .		2
158	Demonstrated Rapid Ballistic Synchronization From Rest of a Hydraulically-Driven Synchronous Generator. IEEE Access, 2018, 6, 75609-75618.	2.6	2
159	Below 1 µV cm ^{â^'1} : determining the geometrically-saturated critical transport current of a superconducting tape. Superconductor Science and Technology, 2021, 34, 085004.	1.8	2
160	Towards a Non-Destructive Method of Mapping the <i>E-J</i> Relation Using Force Decay Measurements on Superconducting Bulks. IEEE Transactions on Applied Superconductivity, 2021, 31, 1-5.	1.1	2
161	Design, Build, and Evaluation of an AC Loss Measurement Rig for High-Speed Superconducting Bearings. Energies, 2022, 15, 1427.	1.6	2
162	Evaluating Common Electronic Components and GaN HEMTs Under Cryogenic Conditions. , 2021, , .		2

Evaluating Common Electronic Components and GaN HEMTs Under Cryogenic Conditions. , 2021, , . 162

#	Article	IF	CITATIONS
163	<title>Mechanical impedance measurements for improved cost-effective process monitoring</title> . , 1999, 3668, 665.		1
164	In-Situ Characterisation of Photo-actuating and Photo-rheological Polymers. Materials Research Society Symposia Proceedings, 2003, 785, 881.	0.1	1
165	F2 laser based fabrication of Fabry-Perot cavities in fused silica and sapphire optical fibres. , 2007, , .		1
166	Rapid synchronisation of fast instantaneous reserves CAES generator. International Journal of Electrical Power and Energy Systems, 2018, 94, 203-212.	3.3	1
167	Feasibility Study on a Fault Current Limiter Consisting of Coated Conductors With Copper Fins for Improved Cooling by Liquid Nitrogen. IEEE Transactions on Applied Superconductivity, 2019, 29, 1-5.	1.1	1
168	Study of Calorimetric Self-Field AC Loss Measurement of HTS Stacks Using FBG Sensors. IEEE Transactions on Applied Superconductivity, 2020, 30, 1-6.	1.1	1
169	Development of a REBCO Magnet for Accelerator. TEION KOGAKU (Journal of Cryogenics and) Tj ETQq1 1 0.784	314 rgBT / 0.1	Overlock 10
170	Mitigation of Shielding-Current-Induced Fields (SCIFs) in HTS Magnets for Accelerator Systems. TEION KOGAKU (Journal of Cryogenics and Superconductivity Society of Japan), 2020, 55, 109-116.	0.1	1
171	Acid-etched Fabry-Perot micro-cavities in optical fibres. Proceedings of SPIE, 2007, , .	0.8	0
172	Palladium based hydrogen sensors using fiber Bragg gratings. Proceedings of SPIE, 2017, , .	0.8	0
173	Performance and Stability Analysis of Hydraulically Driven Synchronous Generators in Power Engineering. , 2018, , .		0
174	Response Time of a Fiber Bragg Grating Based Hydrogen Sensor for Transformer Monitoring. Proceedings (mdpi), 2018, 2, .	0.2	0
175	Cryogenic Sensitivity of Turboelectric Commercial Aircraft with HTS Propulsion Motors. , 2020, , .		0
176	Angle-Dependence of the Levitation Force From a Frustum-Shaped Magnet and Recessed Superconducting Bulk. IEEE Transactions on Applied Superconductivity, 2021, 31, 1-4.	1.1	0
177	Research and Development of the Coil System for a Beam Transport and Irradiation Line. TEION KOGAKU (Journal of Cryogenics and Superconductivity Society of Japan), 2017, 52, 234-243.	0.1	0
178	Simplified Numerical Electromagnetic Field Analysis Method of Coils Wound With Spiral Coated-Conductor Cables. IEEE Transactions on Applied Superconductivity, 2022, 32, 1-5.	1.1	0